Inhibition of the Interaction between class IIa HDAC and MEF2 by Small Molecules

Nimanthi Jayathilaka[1, 2, *], Aidong Han[1, +], Kevin J. Gaffney[3], Raja Dey[1], Jamie A. Jarusiewicz[3], Kaori Noridomi[1,3], Michael A. Philips[1], Xiao Lei[1,2], Ju He[1], Jun Ye[1], Tao Gao[1], Nicos A. Petasis[3, 4, 5], & Lin Chen[1, 2, 3, 4, 6 *]

1. Molecular and Computational Biology, Department of Biological Sciences, University of Southern California, Los Angeles, CA 90089.

2. Genetic, Molecular & Cellular Biology, University of Southern California, Los Angeles, CA 90089.

3. Department of Chemistry, University of Southern California, Los Angeles, CA 90089.

4. Norris Comprehensive Cancer Center, Keck School of Medicine, University of Southern California, Los Angeles, CA 90089.

5. Loker Hydrocarbon Research Institute, University of Southern California, Los Angeles, CA 90089.

6. Key Laboratory of Cancer Proteomics of Chinese Ministry of Health, XiangYa Hospital, Central South University, Changsha, Hunan 410008, China

[*]Correspondence to be addressed to:
Lin Chen, Molecular and Computational Biology, Department of Biological Sciences, University of Southern California, RRI 204c, 1050 Childs Way, Los Angeles, CA 90089, Phone: 213-821-4277, E-mail: linchen@usc.edu

Correspondence may also be addressed to:
Nimanthi Jayathilaka, Molecular and Computational Biology, Department of Biological Sciences, University of Southern California, RRI 216, 1050 Childs Way, Los Angeles, CA 90089, Phone: 858-534-5858, E-mail: jayathil@usc.edu

[+]Present address: The State Key Laboratory of Stress biology, School of Life Sciences, Xiamen University, Xiamen 361005, China

SUPPLEMENTARY DATA

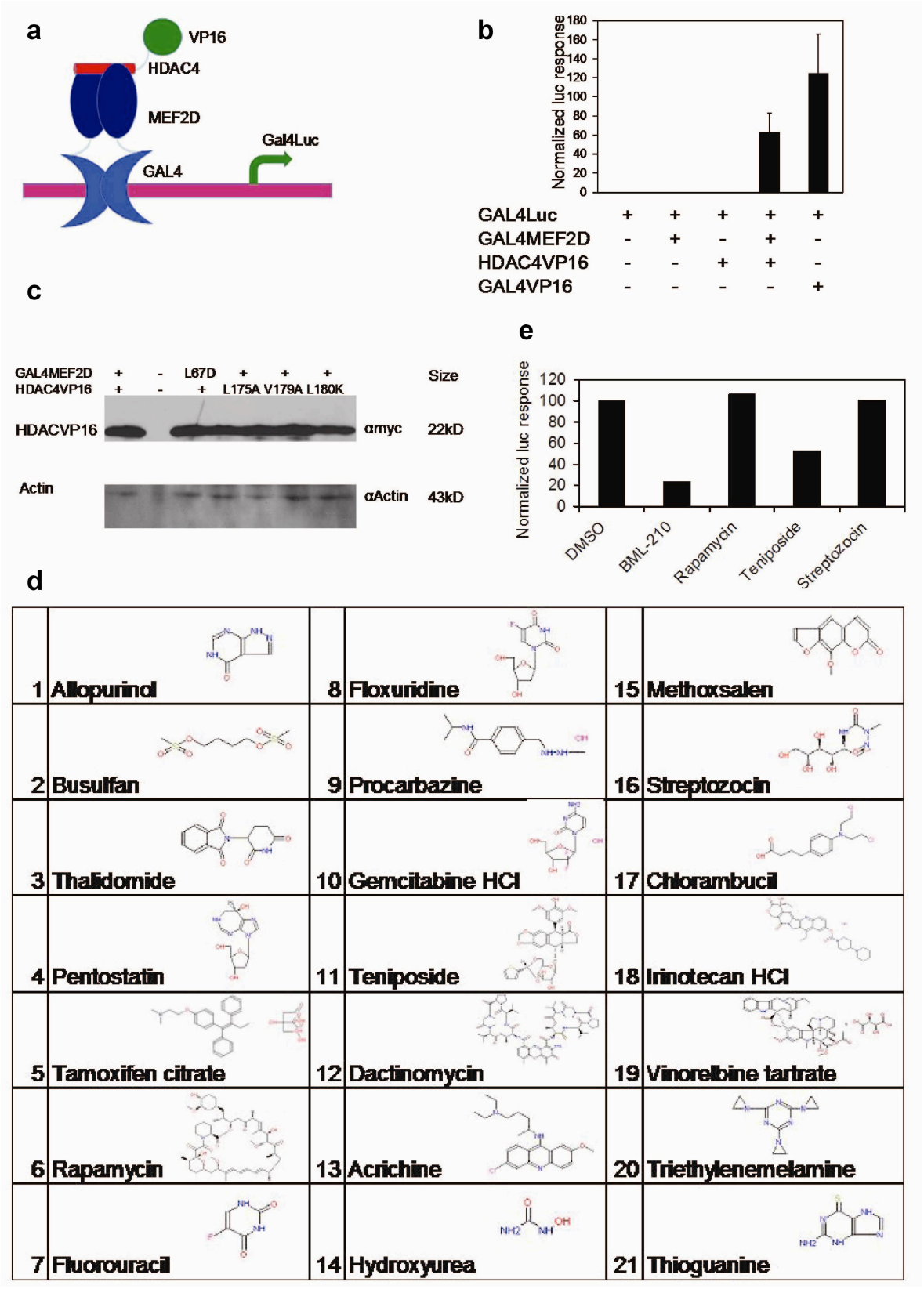

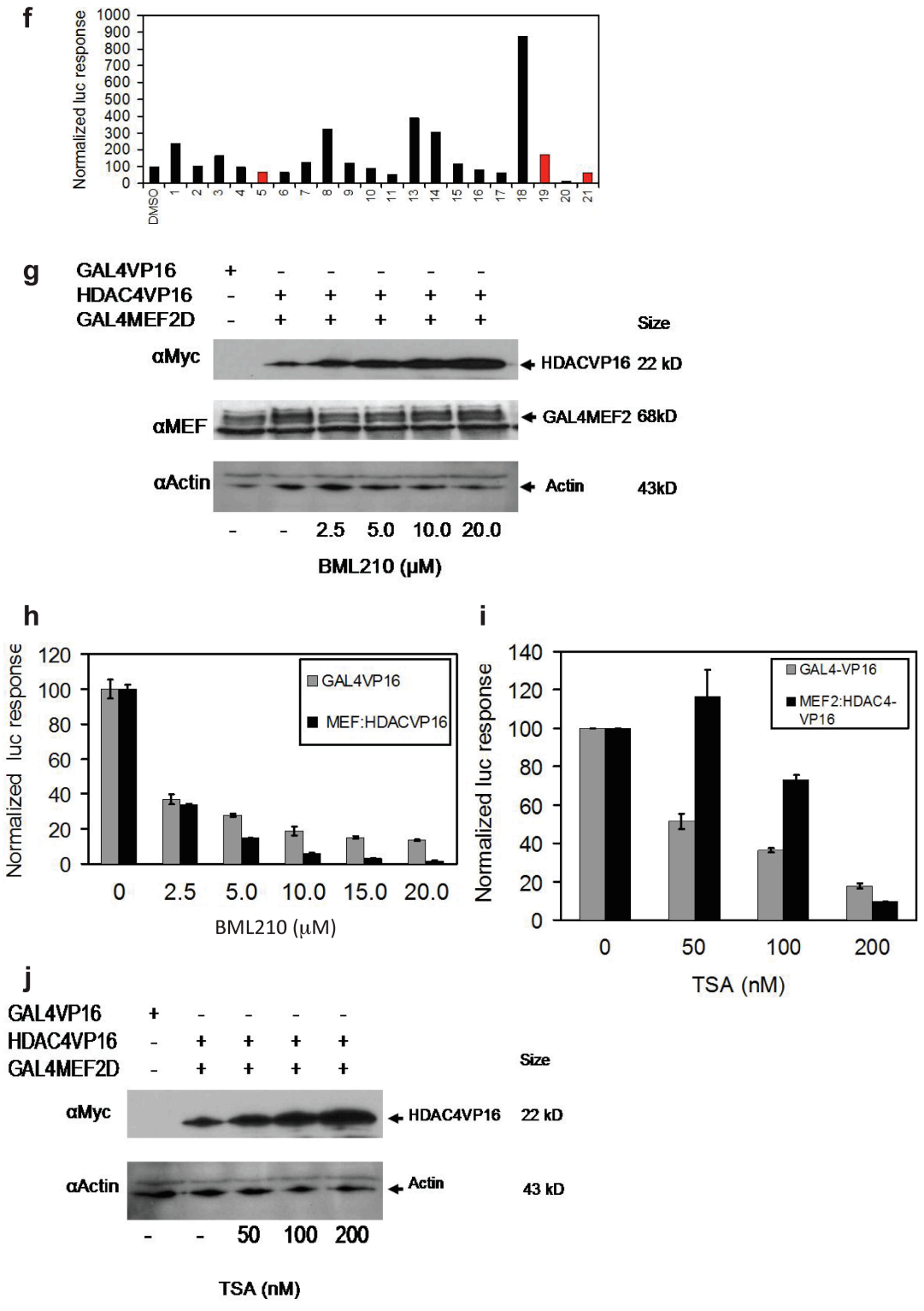

Supplementary Figure S1 Mammalian two-hybrid system for drug screening. (**a**) A

mammalian two-hybrid system: MEF2D (dark blue) was fused with GAL4 -DNA-binding domain (light blue); the MEF2-binding motif of HDAC4 (amino acid residues155-220, red) was fused with VP-16 (green) (**b**) Co-expression of GAL4-MEF2D fusion (GAL4MEF2D) and HDAC4-VP16 fusion (HDAC4VP16) produces a luciferase response comparable to that generated by the positive control GAL4-VP16 fusion (GAL4VP16) in HeLa cells. The relatively stronger signal from GAL4VP16 is probably due to the fact that the activation domain of VP16 is covalently linked to GAL4 whereas in the mammalian two-hybrid assay it is recruited by protein-protein interaction between HDAC4 and MEF2. (**c**) Similar expression level of myc-tagged HDAC4VP16 and the mutants in different experimental conditions was confirmed by western blot. Different combinations of transfection plasmids, including wild type GAL4MEF2D or mutants (L67A and L67D) and HDAC4VP16 and the mutants (L175A, V179A and L180K) are listed above the gel. Actin (lower panel) was used as an internal control**.** (**d***)* Compounds 1 to 21 from the drug screen. (**e**) Luciferase response for the samples treated with compounds 1-22 from the drug screen at 10μM concentration, was measured for the samples that had viable cells. (**f**) The drugs that appeared to be toxic for the cells from the first round of drug treatment were tested in a second round at 2μM concentration and the luciferase response was measured for each. Samples marked in red showed effect on cell viability. Data is presented as a percentage of the DMSO treated sample. In total 92 compounds were tested similarly. (**g**) BML-210 did not decrease the expression of HDAC4-VP16. The expression level of myc-tagged HDAC4-VP16 and GAL4-MEF2D was detected by western blot. Increasing BML-210 concentration induced a slight increase in the expression of HDAC4-VP16. Actin (lower panel) was detected as a

loading control. (**h**) BML-210 non-specifically reduced the normalized reporter signal driven by GAL4-VP16 to a lesser extent than that driven by MEF2:HDAC4-VP16 interaction. The signals from GAL4-VP16 and MEF2:HDAC4-VP16 at zero concentration of BML-210 are set as 100%. (**i**) TSA non-specifically reduced the normalized reporter signal driven by GAL4-VP16 to a greater extent than that driven by MEF2:HDAC4-VP16 interaction up to its IC_{50} value of 100nM. The relatively low inhibition of HDAC4-VP16 reporter signal by TSA compared to BML-210, provides further evidence that the HDAC4-VP16 reporter assay is a sensitive screen for specific interaction between HDAC4 and MEF2D. At high concentration beyond the IC_{50}, TSA also reduced the luciferase response driven by HDAC4-VP16 by approximately 10.6 fold while inhibiting the GAL4-VP16 reporter signal by 5.6 fold resulting in a 1.8 fold inhibition. This inhibition is equivalent to that of BML-210 at its IC_{50} value which inhibited the GAL4-VP16 reporter signal by only 3.6 fold. The signals from GAL4-VP16 and MEF2:HDAC4-VP16 at zero concentration of TSA are set at 100%. (**j**) TSA did not decrease the expression of myc tagged HDAC4-VP16 as detected by western blot. Increasing TSA concentration induced a slight increase of the expression of HDAC4-VP16. Actin (lower panel) was used as loading control.

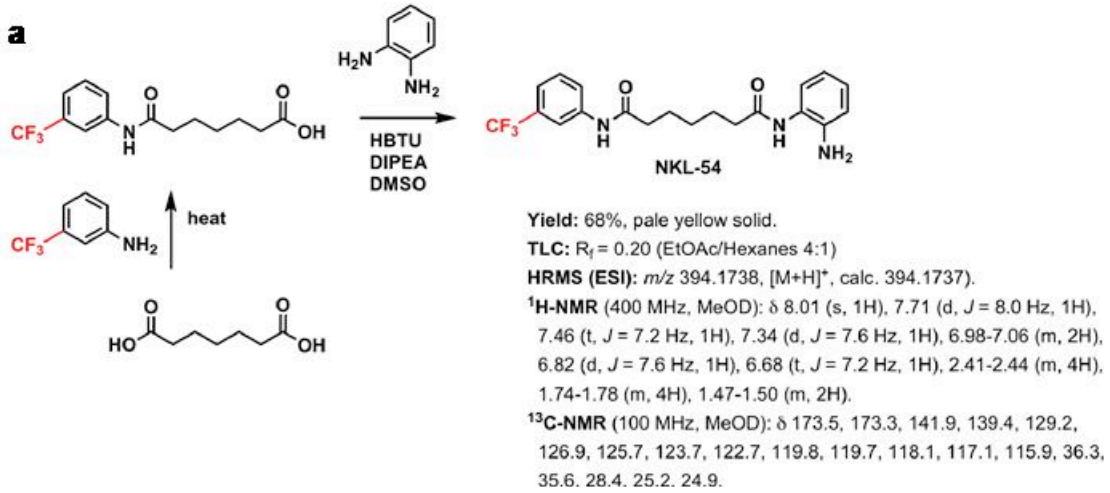

Yield: 68%, pale yellow solid.
TLC: R_f = 0.20 (EtOAc/Hexanes 4:1)
HRMS (ESI): *m/z* 394.1738, $[M+H]^+$, calc. 394.1737).
^{1}H-NMR (400 MHz, MeOD): δ 8.01 (s, 1H), 7.71 (d, *J* = 8.0 Hz, 1H), 7.46 (t, *J* = 7.2 Hz, 1H), 7.34 (d, *J* = 7.6 Hz, 1H), 6.98-7.06 (m, 2H), 6.82 (d, *J* = 7.6 Hz, 1H), 6.68 (t, *J* = 7.2 Hz, 1H), 2.41-2.44 (m, 4H), 1.74-1.78 (m, 4H), 1.47-1.50 (m, 2H).
^{13}C-NMR (100 MHz, MeOD): δ 173.5, 173.3, 141.9, 139.4, 129.2, 126.9, 125.7, 123.7, 122.7, 119.8, 119.7, 118.1, 117.1, 115.9, 36.3, 35.6. 28.4. 25.2. 24.9.

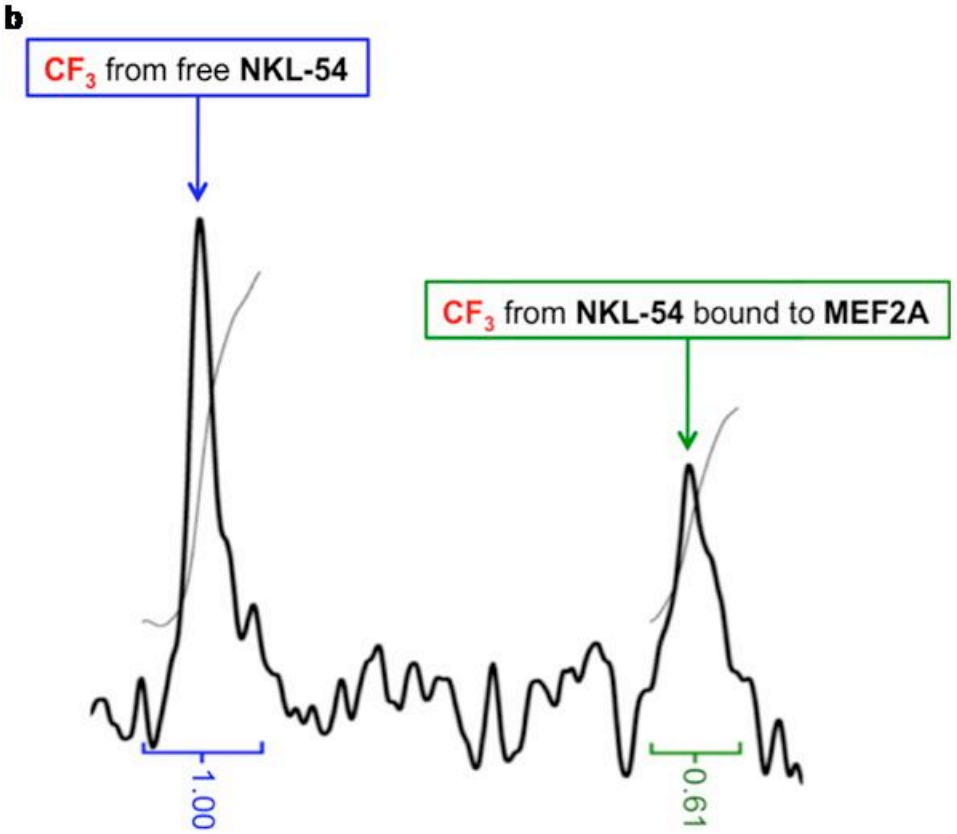

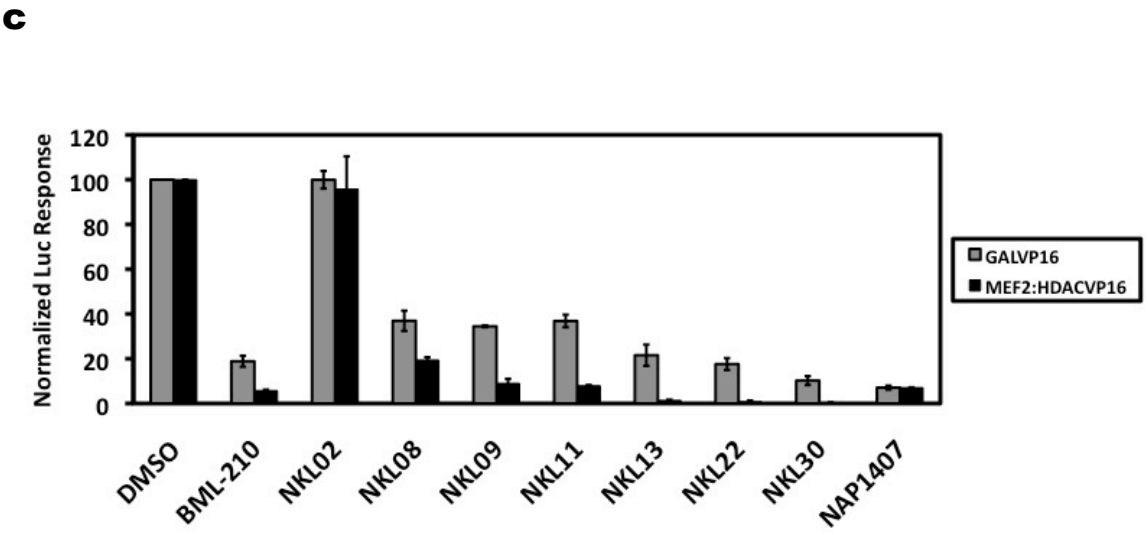

Supplementary Figure S2 ^{19}F NMR with NKL54 (**a**) Synthesis of BML-210 analogs. (**b**) Analysis of NKL54 binding to MEF2 by 470 MHz ^{19}F NMR. In order to determine

the Kd, the concentrations of MEF2A (1-95) and NKL54 were kept low, requiring extended data acquisition time. In the experiment shown, the starting concentrations of both MEF2 and NKL54 were 500 nM, and the relative concentrations of the free and bound NKL54 was estimated by peak integration, shown below the peaks, respectively. Due to the limited signal-to-noise ratio at these concentrations, the Kd (~0.5 μM) is only an estimate, but it is within the expected range for the observed activity. (**c**) Effect of the newly synthesized compounds on the normalized reporter signal (normalized against Renilla Luciferase) driven by MEF2:HDAC4-VP16 interaction vs GAL4-VP16. The signals from GAL4-VP16 and MEF2:HDAC4-VP16 samples treated with DMSO is set at 100%. Transfected cells were treated with 10μM drug or equivalent amount of DMSO.

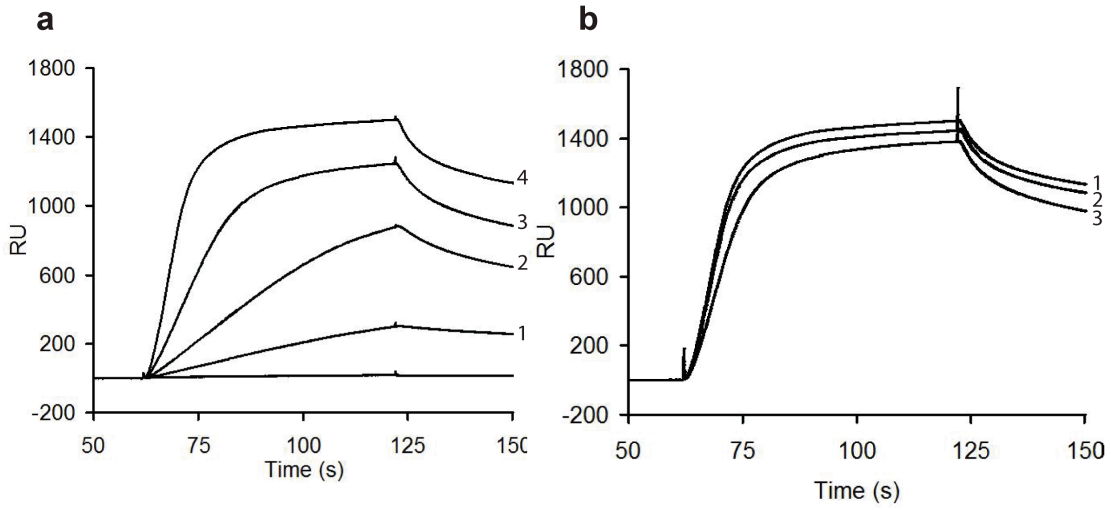

Supplementary Figure S3 Analyzing the binding of HDAC4 to MEF2 and the effect of BML-210 by Surface Plasmon Resonance (SPR) on a Biacore instrument. (**a**) HDAC4 (amino acid residues 155-220) was immobilized on a CM5 sensor chip. MEF2A (1-95) was used as the analyte. The binding of increasing concentrations of MEF2A (traces 1-4) generated a series of sensograms. (**b**) BML-210 inhibited the binding of MEF2 to

HDAC4 immobilized on a Biacore sensor chip instrument. Pre-incubation of MEF2 with increasing amount of BML-210 (traces 1-3) decreased the binding signals.

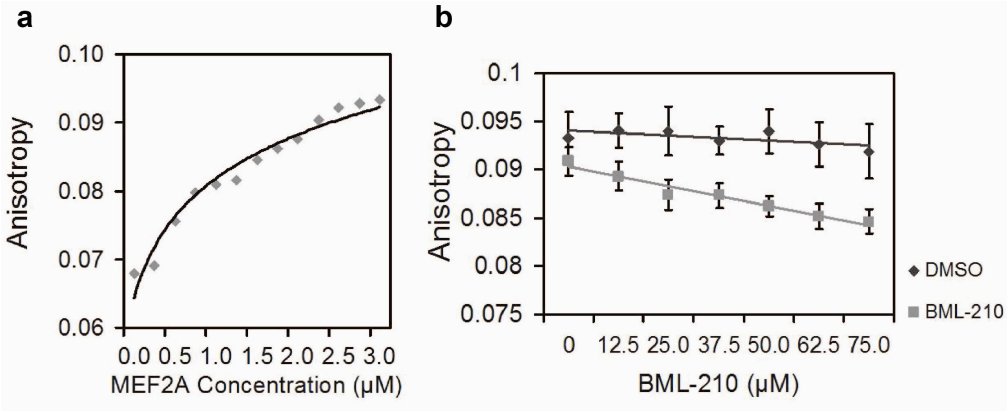

Supplementary Figure S4 Monitoring the binding of MEF2 to HDAC4 and the effect of BML-210 by fluorescence anisotropy. (**a**) Addition of increasing amount of MEF2A (1-95) to IAF-labeled HDAC4 (155-218) led to an increase in fluorescence anisotropy. (**b**) Competition assay by fluorescence anisotropy, addition of increasing amount of BML-210 caused a gradual decay of fluorescence anisotropy, suggesting the displacement of HDAC4 from MEF2 by the small molecule compound.

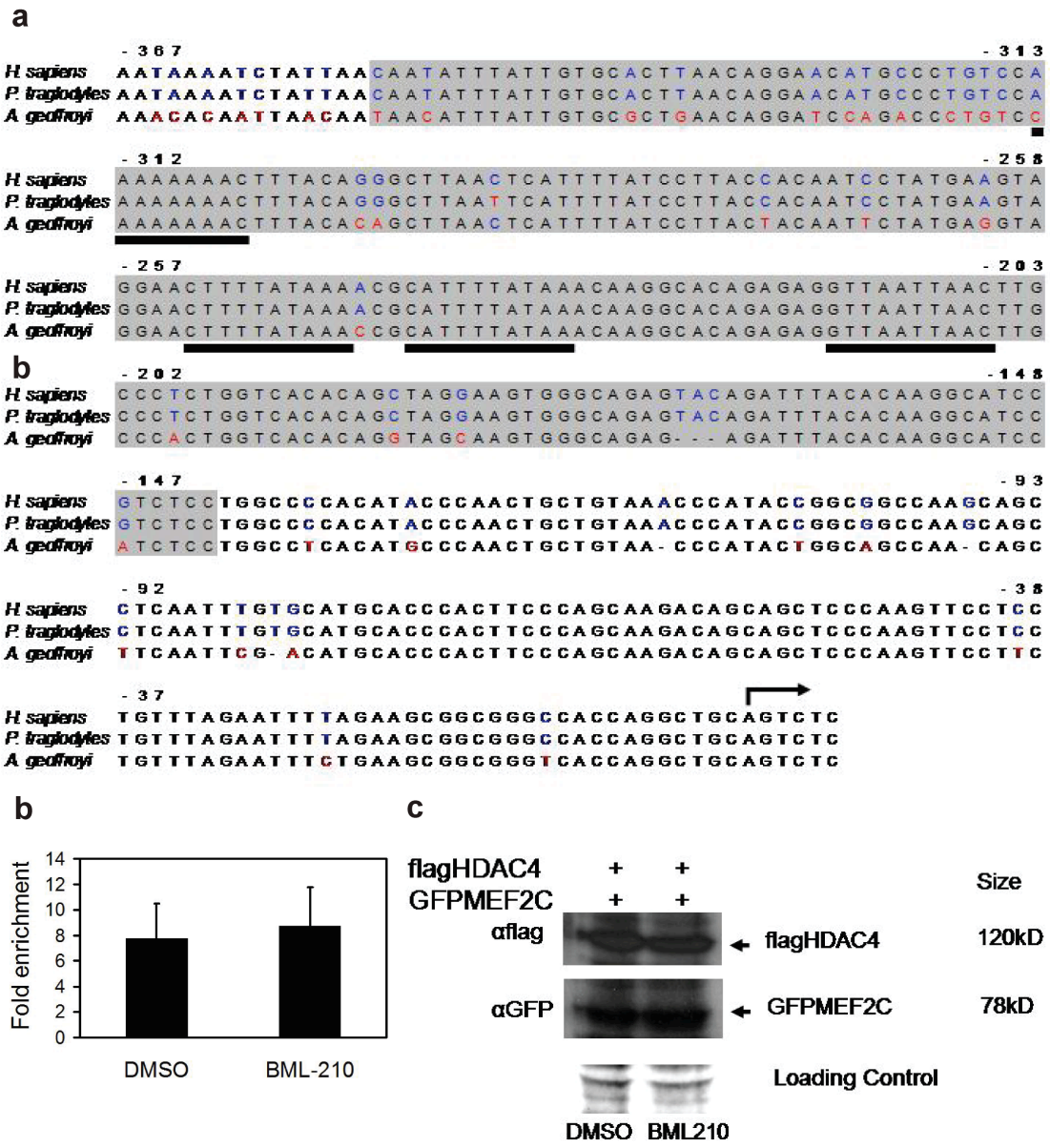

Supplementary Figure S5 Putative MEF2-binding sites in the promoter region of the frataxin gene (FXN). (**a**) Sequences of the MIR (mammalian-wide interspersed repeats,

marked in grey) region of the frataxin promoter from several species are aligned for comparison. This region has been previously reported to contribute significantly to the transcriptional activity (1). Four conserved A/T rich elements that resemble the consensus MEF2 binding sequence are underlined. (**b**) MEF2 is enriched at the *FXN* promoter in FRDA cells. 50 million cells were sonicated for 7 minutes. 5 µg of anti MEF2 (C-21):sc-313 was used for immunoprecipitation. (**c**) Effects of BML-210 on the expression levels of flagHDAC4 and GFPMEF2C in the transfected HeLa cells. Transfected cells were drug treated as indicated with 10μM BML-210 for 6hrs and expression levels of flagHDAC4 and GFPMEF2C was detected by western blot. Coomasie stained membrane was used as a loading control. The expression levels of flagHDAC4 and GFPMEF2C did not change after treatment with BML-210. Therefore, the effect of BML-210 on the HDAC4 occupancy on FXN promoter is not due to any effect on the expression level of flagHDAC4.

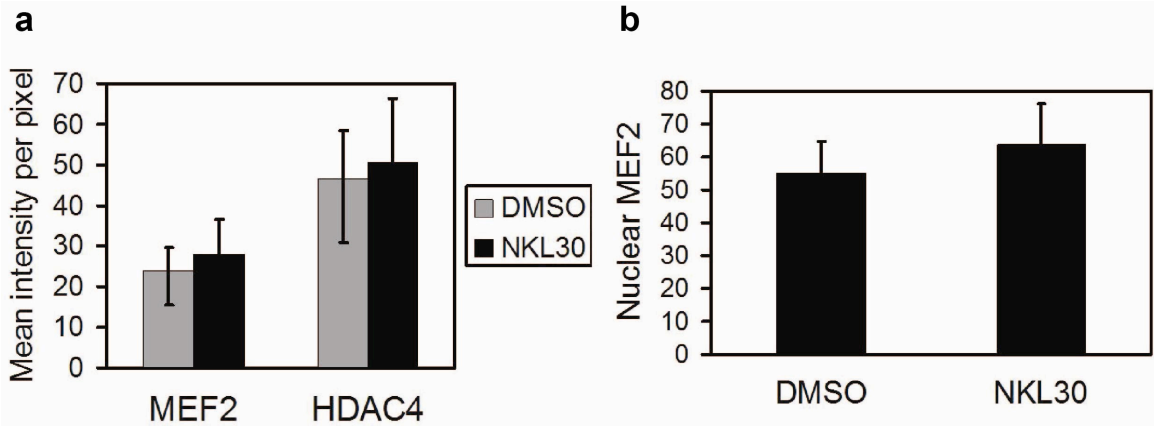

Supplementary Figure S6 Effect of NKL30 on the expression level of MEF2 and HDAC4. (**a**) An area around the nucleus of each cell, including the nucleus was measured. The mean pixel intensity in both MEF2 (P>0.05) and HDAC4 (P>0.2), did not

change (n_{DMSO} =25, n_{NKL30}=25). (**b**) Effect of NKL30 on the level of nuclear MEF2 in COS-7 cells. The nuclear MEF2 level in the NKL30 treated samples did not change ($P>0.25$, n_{DMSO} =25, n_{NKL30}=20)**.**

SUPPLEMENTARY METHODS

Cell Culture, Reagents. HeLa cells and COS-7 cells were maintained in Dulbecco's Modified Eagle Medium (DMEM) containing 10% fetal bovine serum (FBS). NIH 3T3 cells were maintained in DMEM with 10% fetal calf serum. Epstein Barr virus–transformed lymphoblast cell line GM15850 (National Institute of General Medical Sciences (NIGMS) Human Genetic Cell Repository at the Coriell Institute, Camden, New Jersey, USA) was maintained in RPMI 1640 medium with 2 mM L-glutamine and 15% FBS. All cell lines were cultured in a 37°C incubator at 5% CO_2.

Transfections. HeLa and COS-7 cells were transfected using the calcium phosphate precipitation method. NIH 3T3 cells were transfected using Effectene transfection reagent (Qiagen). HeLa cells were harvested for luciferase assays 2 nights after transfection. COS-7 cells and NIH-3T3 cells were harvested one night after transfection. Cells were fixed and harvested for ChIP experiments by drug treating for 6hrs.

For the Luciferase Assays 2ml HeLa cultures and COS-7 cells were co-transfected with 1μg GAL4Luc, 10ng Renilla Luciferase, 1 μg GAL4-MEF2D, 2μg HDAC4-VP16 or 1μg GAL4Luc, 10ng Renilla Lucferase, 250ng GAL4VP16 and

pEXL(His) empty vector as balance DNA to match the amount of DNA in various transfections. NIH 3T3 cells were co-transfected with 100ng GAL4Luc, 10ng Renilla Luciferase, 100ng GAL4-MEF2D, 200ng HDAC4-VP16 or 100ng GAL4-Luc, 10ng Renilla Luciferase, 50ng GAL4VP16 and 250ng pEXL(His). For the ChIP experiments, 10ml HeLa cultures were transfected with either 12.5μg flag HDAC4FL and GFP-MEF2CFL each or 25μg flagMEF2CFL. Expression and colocalization of MEF2 and HDAC4 in ChIP samples was confirmed by observing the punctuated spots in the nucleus (2). For the control ChIP experiments with only flagHDAC4FL, that were performed to confirm MEF2 mediated HDAC4 recruitment to the promoter, pEGFP-C1(BD Biosciences Clontech) was used to match the total amount of transfected DNA and to confirm efficient transfection.

Plasmid Constructs. GAL4MEF2DFL, flagHDAC4FL, GFPMEF2CFL and flagMEF2CFL were kindly provided by Dr Xiang-Jiao Yang, McGill University Health Center, Montreal, Canada. HDAC4VP16 was generated by PCR amplifying and cloning MYC tagged human HDAC4 (155-220), N terminal to VP16 in a modified pEGFP-N2 (BD Biosciences Clontech) vector without the GFP (pEXLVP16). GAL4Luciferase and Renilla Luciferase (pRL-TK) and GAL4VP16 were provided by Dr. Xuedong Liu, Department of Chemistry and Biochemistry, University of Colorado at Boulder. For the mutational analysis in the mammalian two hybrid system, mammalian expression constructs HDAC4L175A(155-220)VP16 and HDAC4V179A(155-220)VP16 were generated by pcr amplification of previously reported HDAC4 mutants L175A and V179A and cloning in to the pEXLVP16 vector. HDAC4L180K(155-220)VP16 was

generated by using the QuikChange II Site Directed Mutagenesis Kit (Catalog #200523, Stratagene) according to kit protocol (3). MEF2A (1-95) was generated as described previously (4). MEF2A (1-78) was generated by cloning human MEF2A residues 1-78 in to PET30b vector. mycHDAC4(155-220) was previously reported by Han *et al,* 2005. mycHDAC4(155-218) was generated by cloning MYC tagged HDAC4(155-218) in to pE-Sumo vector (SUMO Pro), C terminal to the Sumo tag.

Western Blot Analysis. Effect of drug treatment on HDAC4-VP16 expression in the luciferase assay samples was detected by western blot analysis using anti c-MYC(9E10):sc-40 (1:200 Santa Cruz Biotechnology, Santa Cruz, CA) antibody. GAL4-MEF2D expression was detected using anti MEF2 (C-21):sc-313 (1:200 Santa Cruz). Actin expression was using anti Actin (C-2):sc-8432 (1:200 Santa Cruz). Effect of drug treatment on flagHDAC4 was detected using mouse monoclonal anti-FLAG M2:F3165 (1:5000 Sigma-Aldrich, St. Louis, MO). GFP-MEF2C expression was detected using living Colors Full-Length A.v. rabbit polyclonal Antibody against GFP (1:2000 Clontech laboratories, Inc., mountain View, CA). Transfected 2ml cell cultures were harvested by active lysis with 50 μl 1X Passive Lysis Buffer (Promega, Madison, WI) according to manufacturer protocol. Luciferase activity was confirmed for relevant samples.

Protein Expression and Purification. All proteins were expressed in *Escherichia coli* BL21(DE3)pLysS at 25°C over night. MEF2A (1-95) was purified as previously indicated (4). MEF2A (1-78) was purified following the protocol for MEF2A (1-95). Myc-HDAC4 (155-220) was purified by Nickel affinity purification followed by Mono Q

cation exchange (GE healthcare). Sample was collected from the unbound fractions and further purified using Mono S anion exchange (GE Health care). Sample was desalted for future experiments by diluting in 10mM HEPES pH 7 and concentrating using a Biomax 5K cutoff filter (Millipore). mycHDAC4 (155-218) was purified by Nickel affinity purification and cleaving the Sumo tag using Sumo Protease 1. Collected sample was affinity purified on a Mono Q column (GE Healthcare).

Surface plasmon resonance using BIAcore. Binding experiments were performed on a BIAcore T100 biosensor system, GE Healthcare (NanoBiophysics Core Facility, USC, CA) at 25°C. mycHDAC4(155-220) protein (160μl of 1.4μM polypeptide in 10mM HEPES, pH 7) was coupled to the sensor surface of a CM5 Biacore sensor chip (GE Healthcare) using amine coupling with N-hydroxy-succinimide/N-ethyl-N-(dimethylamino-propyl)carbodiimide (NHS/EDC) chemistry as recommended by the manufacturer (GE Healthcare). 300 resonance units were immobilized on the surface and the remaining activated groups on the surface were inactivated with 1mM ethanolamine. For control experiments, one sensor surface was treated as above in the absence of HDAC4 protein. Interaction experiments between HDAC4 and MEF2A (1-95) protein were carried out with MEF2A concentrations ranging from 37.5nM to 300nM at a constant flow rate of 50 μl/min using 1XPBS-EPD buffer (1xPBS pH 7.4, 3mM EDTA, 0.05% surfactant P20, 5% DMSO) as running buffer. Sample buffer and running buffers were matched as close as possible. Between injections, the sensor surface was regenerated with 25mM NaOH for 15 seconds at a flow rate of 10μl/min followed by a second regeneration step using running buffer (1XPBS-EPD) at a flow rate of

50μl/minute for 2 minutes. Competitive binding of BML-210 to MEF2A was detected with 300nM MEF2A incubated with increasing concentration of BML-210 (diluted from the 10 mM DMSO stock to 200μM to 500μM) at room temperature for 30 minutes. Under these experimental conditions, the concentration of BML-210 in aqueous solution seemed to decrease gradually after dilution from the DMSO stock, probably due to limited solubility of BML-210. This was confirmed by NMR and by the observation of oil droplet (indication of phase separation) in the solution. Samples were run over the sensor surface and regenerated as indicated above. 20X stock solutions of each concentration of BML-210 was dissolved in 100% DMSO in order to avoid DMSO concentration changes. 5% DMSO was added to the control samples. Samples were incubated in 1XPBS-E0.01%P buffer (1XPBS pH7.4, 3mM EDTA, 0.01% surfactant P20) and the amount of P20 was adjusted to 0.05% to match the running buffer.

5-IAF labeling and fluorescence anisotropy. mycHDAC4 (155-218) was fluorescent labeled at the cysteine residue 194 using 5-iodoscetamidofluorescein (5-IAF)(Pierce, Rockford, IL). 1M DTT was added to approximately 0.5mg/ml mycHDAC4 (155-218) in 600-700μl MonoQ buffer (20mM Tris HCl pH8.5, 1mM EDTA, 1mM DTT, 100mM NaCl) to a final concentration of 20mM and incubated at room temperature for 2hrs, rotating in the dark to reduce the disulfide bonds. Sample was then diluted 20 times using MonoQ buffer to bring the DTT concentration below 1mM and concentrated back to approximately 1ml volume using Amicon 3K cut off filter (Millipore) in 4°C. The pH of the sample was adjusted to pH8.5 by adding 1/10th volume 0.5M Tris HCl, pH 8.5. 100mM 5-IAF dissolved in 100% DMF was added to the sample to a final concentration

of 3mM and incubated in the dark in 4°C rotator ON. Sample was then denatured in 6M urea to release the excess 5-IAF and dialyzed using 1K cutoff dialysis tubing in MonoQ buffer ON at 4°C. Exchange buffer for dialysis was changed and the sample was dialyzed for another 8hrs. Sample was then concentrated using Amicon 3K cutoff filter and the amount of label was measured by measuring the absorbance at 491nm. The sample concentration was measured by Bradford assay and the degree of labeling was calculated for estimating the amount of labeled protein. Fluorescence anisotropy was measured using QuantaMaster QM-4SE Spectrofluorometer , Photon Technology International (NanoBiophysics Core Facility, USC, CA) at an excitation wavelength of 495nm and emission wavelength of 520nM. Increasing concentrations of 80 μM MEF2A (1-95) was titrated at a concentration range between 250nM to 3μM to 250nM fluorescence (FITC) labeled mycHDAC4(155-218) (HDAC4-5IAF) to obtain a saturated binding curve. The assay was performed in 1XPBS, pH7.4. Once signal saturation was reached increasing concentrations of 10mM BML-210 in 100% DMSO was added to the sample in a concentration range between 12.5μM to 75μM.

Structure determination and analysis. The crystals diffracted to 2.40 Å and the data were processed at 2.43 Å. Data were reduced with the program HKL2000 (5). Structure determination and refinement were carried out with the crystallography software suit PHENIX (6). Model building and refinement were performed with O (7). The illustration was made with PyMOL (The PyMOL Molecular Graphics System, Version 1.2r3pre, Schrödinger, LLC.). There were two complexes in the asymmetric unit. While the density of BML-210 in one complex is clearly visible at 0.7-1.0 sigma, the density of

BML-210 in the second complex is weaker, presumably due to different crystal packing environment. The occupancy of BML-210, estimated by the electron density in simulated omit map, is highly dependent on the protocol of complex preparation and crystallization conditions. This is probably due to the limited solubility of BML-210 in aqueous solution, which could be affected by buffer conditions used to grow crystals. The thin-plate shape of the crystals also contributed to the variability of diffraction quality. As such, the best data set was from a crystal collected at the home source, which was lost during recovery. Other data sets collected with different crystals at a synchrotron source were not as good because of the high mosaicity or smearing spot shape. The binding of BML-210 to MEF2 in the crystal is also affected by crystal packing, which led to the asymmetric binding of the compound to the MEF2 dimer.

Immunocytochemistry. COS-7 cells were cultured on poly-D-Lysine coated cover-slips in 6 well plates and drugged after incubating ON to allow surface attachment. Cells were fixed with PFA after treatment with 10 μM drug ON and immunocytochemistry was performed according to previously published method (8) using a block solution containing 3% bovine serum albumin, 0.1% Triton X-100 in PBS. Primary antibodies were diluted as following in block solution and incubated with sample for 45 minutes: mouse anti-MEF2(B4) (Santa Cruz) 1:50, rabbit anti-HDAC4 (Coriell) 1:500. Secondary goat antibodies were conjugated to Alexa 488, 594 fluorophores (Invitrogen) 1:1000.

SUPPLEMENTARY REFERENCES

1. Greene, E., Entezam, A., Kumari, D. and Usdin, K. (2005) Ancient repeated DNA elements and the regulation of the human frataxin promoter. *Genomics*, **85**, 221-230.
2. Chan, J.K., Sun, L., Yang, X.J., Zhu, G. and Wu, Z. (2003) Functional characterization of an amino-terminal region of HDAC4 that possesses MEF2 binding and transcriptional repressive activity. *J Biol Chem*, **278**, 23515-23521.
3. Han, A., He, J., Wu, Y., Liu, J.O. and Chen, L. (2005) Mechanism of recruitment of class II histone deacetylases by myocyte enhancer factor-2. *J Mol Biol*, **345**, 91-102.
4. Wu, Y., Dey, R., Han, A., Jayathilaka, N., Philips, M., Ye, J. and Chen, L. Structure of the MADS-box/MEF2 domain of MEF2A bound to DNA and its implication for myocardin recruitment. *J Mol Biol*, **397**, 520-533.
5. Otwinowski, Z. and Minor, W. (1997) Processing of X-ray Diffraction Data Collected in Oscillation Mode. *Methods in Enzymology*, **276**, 307-326.
6. Adams, P.D., Afonine, P.V., Bunkoczi, G., Chen, V.B., Davis, I.W., Echols, N., Headd, J.J., Hung, L.W., Kapral, G.J., Grosse-Kunstleve, R.W. *et al*. (2010) PHENIX: a comprehensive Python-based system for macromolecular structure solution. *Acta Crystallogr D Biol Crystallogr*, **66**, 213-221.
7. Kleywegt, G. and Jones, T.A. (1994) In Bailey, S., Hubbard, R. and Walker, D. (eds.), *From First Map to Final Map Model*, Warrington: Daresbury Laboratory.
8. Lewis, T.L., Jr., Mao, T., Svoboda, K. and Arnold, D.B. (2009) Myosin-dependent targeting of transmembrane proteins to neuronal dendrites. *Nat Neurosci*, **12**, 568-576.